360°-Beam-Steering Low-Side-Lobe Time Reversal Microwave Power Transfer by Superposition of Multiple Weighted Radiation Modes

Lin Hu, Josep Parron, Pedro de Paco, *Senior Member, IEEE,* Deshuang Zhao, *Member, IEEE*, Bing-Zhong Wang, *Senior Member, IEEE*

***Abstract*—This letter proposes a 360°-beam-steering low-side-lobe time reversal microwave power transfer (TR-MPT) method. The beam steering is implemented by only one circular patch antenna fabricated with multiple feeding ports. The multiple feeding ports are designed to stimulate different radiation modes and their combinations to steer the beam within 360° in the azimuth plane. To depress the sidelobe levels and enhance the beam gain, a disc-top-loaded monopole antenna is added at the center of the patch antenna, which is used to excite an additional mode out of phase with the maximal sidelobe but in phase with the main lobe. Finally, time reversal (TR) is adopted for optimally weighting the stimulated modes and focusing the power beam adaptively to the desired receiver. A prototype of the TR-MPT system based on the proposed method is established. The experiments demonstrate that the new method can not only adaptively focus the power at the receiver placed at any azimuth angle within 360°, but also achieve a low sidelobe level of smaller than -8.57 dB under a 0.7-wavelength aperture. Additionally, the power transferred to the receiver at different angles has a small fluctuation of less than 0.7 dB.**

***Index Terms*—microwave power transfer, low side lobe, beam steering, time reversal.**

I. INTRODUCTION

WIRELESS power transfer (WPT) technology delivers power wirelessly to electronic devices, allowing them to work forever without cables or battery replacement [1-3]. Different from near-field WPT methods, microwave power transfer (MPT) employs the radiation electromagnetic beams formed by the microwave signals to transmit wireless energy, which offers the unique advantages of long energy transmission distance and no strict alignment of transmitters and receivers [4-6]. Recently, MPT has begun to be used in indoor scenes by virtue of auto-tracking performance [7-14]. In practical scenarios such as smart factories and smart homes, devices (like sensors, RFID tags, wireless headphones or smart bracelets) will be distributed at different angles of the transmitter, making the wide-angle MPT a research focus.

For the traditional MPT, a linear array of patch antennas spaced at $\lambda/2$ intervals is mainly used as the transmitter [4-14]. This makes the size of the transmitting antenna large (more than 2 λ), the available angular range small (generally within $\pm 45°$), and the maximum power of the beam to fluctuate greatly in different target angles (more than 3dB). In contrast, the omnidirectional pattern of a single monopole can be used to implement 360° MPT, but this pattern cannot form a power beam to achieve MPT with selectivity and safety [15]. Similarly, the antenna array consisting of the multiple monopoles generates a mirrored power beam in rear hemisphere.

Recently, a 360° beam steering antenna have been realized based on the superposition of four high-order radiation modes of the circular patch antenna [16]. However, this antenna produces high level side lobes when forming the power beam, resulting in poor safety and electromagnetic compatibility MPT system. It is worth noting that this small-aperture antenna (less than 0.7λ) is difficult to achieve low side lobes through the traditional Chebyshev weighting method or Taylor weighting method. In addition, the position information of the users is difficult to obtain in practical application scenarios, so the power beam cannot be auto-focused on the user [17-18].

Therefore, inspired by the 360° beam steering antenna and the auto-focus characteristics of TR, this paper proposes a 360° -beam-steering low-side-lobe time reversal microwave power transfer (TR-MPT) system based on the superposition of multiple weighted radiation modes in phase. The relationship between the power beam (the main lobe) and the side lobes is analyzed, which lays a theoretical foundation for the method to reducing the level of side lobes. A disc-loaded folding monopole antenna was chosen to redesign a 5-port compact antenna. The experimental results demonstrate that the proposed approach can not only adaptively focus the power beam at the receiver of any steering angle within 360°, but also achieve a low side lobe level.

II. 360°-BEAM-STEERING LOW-SIDE-LOBE TR-MPT

A. Weighted Multi-Modes Superposition with Low Side Lobes

Manuscript received Month xx, 2xxx; revised Month xx, xxxx; accepted Month x, xxxx. This work was supported in part by 2021 Medical Oncology and Engineering Innovation Fund project (no. ZYGX2021YGCX008), 2023 Radiation Oncology Key Laboratory of Sichuan Province, and the Universitat Autònoma de Barcelona. (*Corresponding author: Deshuang Zhao.*)

Lin Hu is with the School of Physics, University of Electronic Science and Technology of China, Chengdu, 611731, China, and also with the Department of Telecommunications and Systems Engineering, Universitat Autònoma de Barcelona, Barcelona, 08193, Spain (email: 202011120510@std.uestc.edu.cn).

Deshuang Zhao and Bing-Zhong Wang are with the School of Physics, University of Electronic Science and Technology of China, Chengdu, 611731, China (email: dszhao@uestc.edu.cn; bzwang@uestc.edu.cn).

Deshuang Zhao is also with the Yangtze Delta Region Institute of University of Electronic Science and Technology of China, Huzhou 313000, China.

Josep Parron and Pedro de Paco are with the Department of Telecommunications and Systems Engineering, Universitat Autònoma de Barcelona, Barcelona, 08193, Spain (email: Josep.Parron@uab.cat; pedro.depaco@uab.cat).

A 360°-beam-steering radiation beam was realized in our previous work through the superposition of four radiation modes [16], but the level of side lobes is high. In order to depress the level of side lobes, we analyze the superposition process to obtain the relationship between the power beam and the side lobes, which lays a theoretical foundation for the method to reducing the level of side lobes.

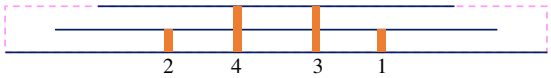

Fig. 1 Cross-sectional diagram of the 4-port antenna with high side lobes [14].

Taking the target angle as $\varphi_{\text{aim}}= 90°$ as an example, working principle of our previous work is that two orthogonal TM31 modes (port 1 and port 2 in Fig.1) form the $\cos(3(\varphi-\varphi_{\text{aim}}))$ pattern and the other two orthogonal TM21 modes (port 3 and port 4 in Fig.1) form the $\cos(2(\varphi-\varphi_{\text{aim}}))$ pattern [16]. The final result obtained from superposition of these modes can be described as

$$\cos(3(\varphi-\varphi_{\text{aim}}))+\cos(2(\varphi-\varphi_{\text{aim}}))= 2\cos(2.5(\varphi-\varphi_{\text{aim}}))\cos(0.5(\varphi-\varphi_{\text{aim}})) \quad (1)$$

Fig.2 a and b show the magnitude and phase of the radiation pattern formed in the target angle. From Fig. 2a, the final pattern consists of 1 main lobe and 4 side lobes. The amplitude of two side lobes with high amplitude and the amplitude of two side lobes with low amplitude are represented as *A*_high and *A*_low, respectively.

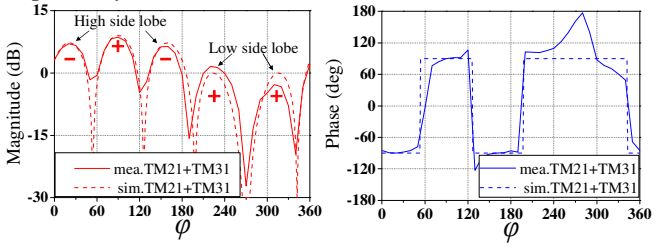

Fig. 2 Simulated and measured radiation pattern formed by TM21 and TM31 modes. (a) Magnitude. (b) Phase.

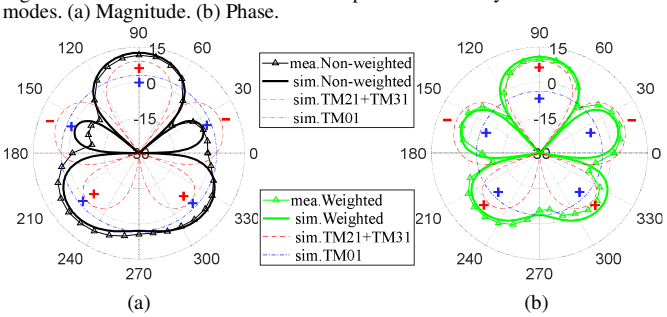

Fig. 3 Simulated and measured radiation pattern formed by TM21, TM31 and TM01 modes. (a) Non-weighted superposition. (b) Weighted superposition.

From Fig. 2, it can be seen that the two side lobes with high level are out phase with the main lobe. This inspired us to add an omnidirectional mode TM01 to increase the level of the main lobe and decrease *A*_high as shown in Fig.3a. However, there are still high-level sidelobes as shown in Fig.3a because *A*_low increases. The cause of this phenomenon is the two side lobes with low level are in phase with the main lobe. Therefore, the omnidirectional mode TM01 not only reduces *A*_high but also increases *A*_low. This mechanism motivates us to set the amplitude of TM01 mode as

$$A_{\text{opt}} = (A\_\text{high}-A\_\text{low})/2 \quad (2)$$

so that the level of the reduced high-level side lobe is equal to the level of the increased low-level side lobe, resulting in the lowest side lobe level as shown in Fig.3b.

B. 5-Ports Compact Antenna

Thanks to the field distribution of the TM31 and TM21 modes in the central region of the circular patches is zero [16][19], we implemented the TM01 mode by adding a monopole antenna to the center [20]. However, the unload monopole antenna made the antenna profile too high, and in order to obtain a more compact antenna, we adopted a disc-top-loaded monopole antenna to achieve the TM01 mode [21].

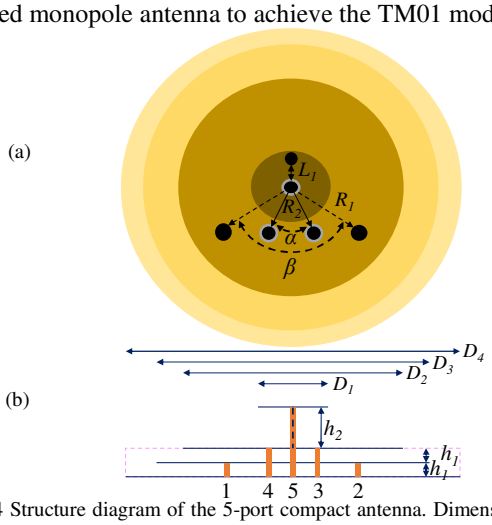

Fig. 4 Structure diagram of the 5-port compact antenna. Dimensions (in mm) are: D_1 = 17.9, D_2 = 56.4, D_3 = 74, D_4 = 85, h_1 = 3, h_2 = 10.9, R_1 = 20, R_2 = 14, L_1 = 6.2. Angles (in degrees) are α = 45, β = 90. (a) Upper view. (b) Side view.

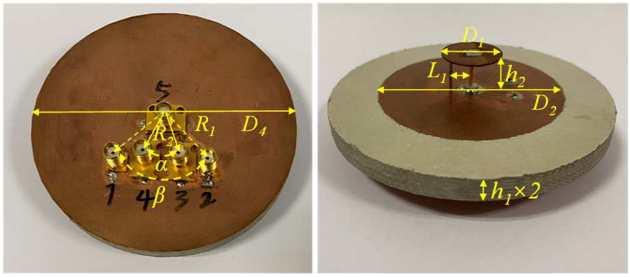

Fig. 5 Manufactured 5-port compact antenna. (a) Bottom view. (b) Top view.

Fig. 4 shows the structure diagram of the redesigned 5-port compact antenna using TACONIC TRF 45 substrate (ε_r = 4.5, $\tan\delta$ = 0.0037). The cross-sectional size of the antenna is π ×4.25^2 cm^2, and the height has been reduced from 36 mm to 16.9 mm. The manufactured 5-ports compact antenna is shown in Fig.5. The S-parameters of each antenna port are tested and plotted in Fig. 6. All five ports achieve good impedance matching at 2.406GHz. The pattern of each port of the antenna was also tested, as shown in Fig. 7. Port 1 and port 2 implement the quadrature TM31 radiation modes, port 3 and port 4 implement the quadrature TM21 radiation modes, and port 5 implements the omnidirectional TM01 radiation mode.

C. 360°-Beam-Steering Low-Side-Lobe TR-MPT Method

The TR technology with space-time focusing characteristics

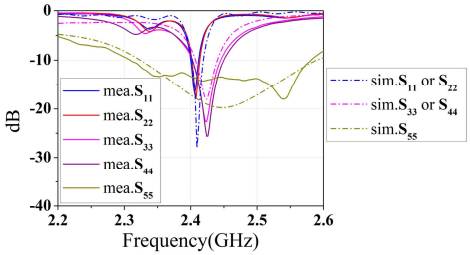

Fig. 6 Simulated and measured S-parameters of the 5-ports compact antenna

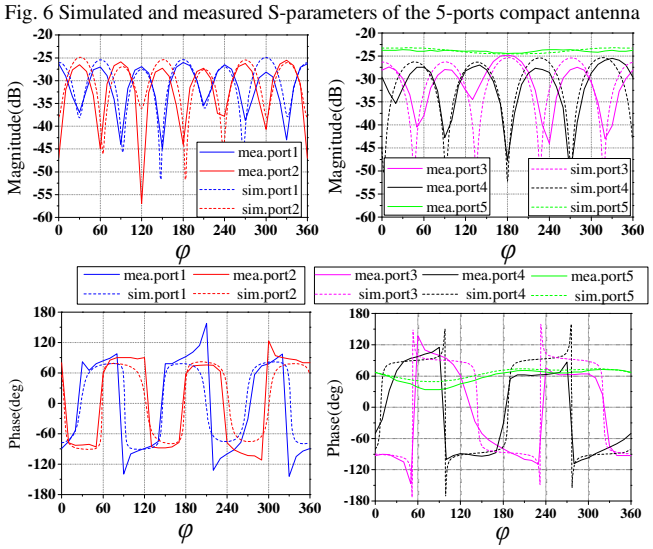

Fig. 7 Simulated and measured magnitude and phase of radiation modes of the 5-ports compact antenna

can adaptively focus the power beam at the receiver [7]. The weighted multi-mode superposition can achieve the steering angle of an range of 360° and the low side lobe levels as described in section II.A. Therefore, the TR technology combined with the weighted multi-mode superposition can achieve excellent performance with 360° beam steering, low-side-lobe and auto-focus MPT using the following algorithm:

Step 1: the transmitter receives the pilot signal from the receiver to obtain the channel information between the transmitter with 5-ports antenna and the receiver as follows:

$$\boldsymbol{h}^{\mathrm{T}} = [h_1, h_2, \ldots, h_5] \subset \mathbb{C}^{1\times 5} \tag{3}$$

where h_{i} represents the channel information between the i-th port of transmitter and the port of receiver, $(\,)^T$ denotes the transpose operation.

Step 2: After TR operation, the transmission signal of the traditional TR-MPT is obtained as:

$$\boldsymbol{X}_{\mathbf{init}} = \boldsymbol{h}^{\mathrm{H}} = [h_1^*, h_2^*, \ldots, h_5^*] \subset \mathbb{C}^{5\times 1} \tag{4}$$

where $(\,)^*$ denotes the conjugate operation, $(\,)^H$ denotes the conjugate transpose operation.

The TR combine weighted multi-mode superposition method obtains the low-side-lobe transmission signal as

$$\boldsymbol{X} = \boldsymbol{diag}(\boldsymbol{w}) \cdot \boldsymbol{h}^{\mathrm{H}} \tag{5}$$

where $\boldsymbol{diag}(\,)$ denotes the operator converting a vector to a diagonal matrix, $\boldsymbol{w} = \left[\mathbf{1}, \mathbf{1}, \mathbf{1}, \mathbf{1}, (\boldsymbol{A}_{\mathbf{opt}}/\,|\boldsymbol{h}_5|)\right]$ represents the weighted vector that achieves the lowest side lobe level.

Step 3: The low-side-lobe transmission signal $\boldsymbol{X}$ is fed to the transmitting antenna.

Fig.8 shows the summarized flow chart of the proposed 360°-beam-steering low-side-lobe TR-MPT method.

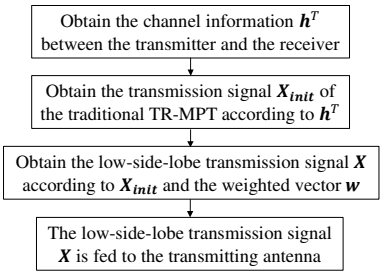

Fig. 8 The summarized flow chart of the 360°-beam-steering low-side-lobe TR-MPT method

III. Experimental Results

A. Performance of the 360°-Beam-Steering Low-Side-Lobe TR-MPT Method

To evaluate the performance of the 360°-beam-steering low-side-lobe TR-MPT method proposed in this letter, we conducted experiments in a microwave anechoic chamber with a roller. According to the measured S-parameters of the 5-ports compact antenna, we chose 2.406 GHz as the system operating frequency.

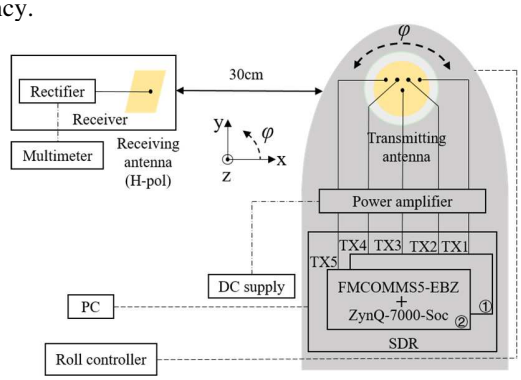

Fig. 9 Schematic of the MPT

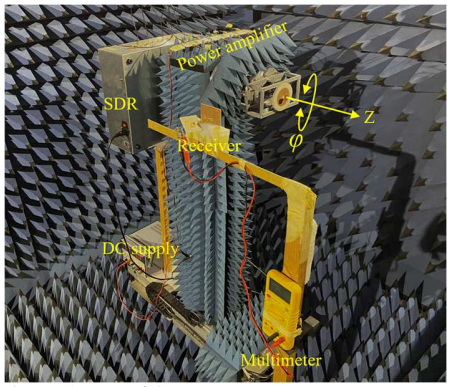

Fig. 10 Experimental setup of the MPT

Fig. 9 shows a schematic of the experiment. Based on the channel information obtained from *Step 1* of section II.C, software defined radio (SDR) obtains the low side lobe transmission signal $\boldsymbol{X}$ by controlling the amplitude and phase. The low side lobe transmission signal $\boldsymbol{X}$ is amplified by the power amplifier and fed into the transmitting antenna. As a consequence, the power beam is auto-focused on the receiver by virtue of space-time focusing characteristic of TR. The transmitting antenna fixed on the roller rotates 360° and records the DC power output by the receiver during the 360° rotation. Thus, the power distribution results in the range of 360° are

obtained.

Fig. 10 shows the experimental setup. The phase control accuracy and amplitude control accuracy of the SDR are set to 1° and 0.1dB, respectively. The gain of the power amplifier is 28dB. The maximum transmit RF power of each port of the transmitting antenna is 24 dBm. The receiver consists of a receiving antenna and a rectifier. The receiving antenna has a measured gain of 6.8 dBi and a measured S11 parameter of -17.8dB at the operating frequency. The rectifier is for converting the received RF power to dc power. The maximum conversion efficiency of the rectifier is 74.6%, which achieves at an input RF power of 10 dBm with a load of 5100 Ω.

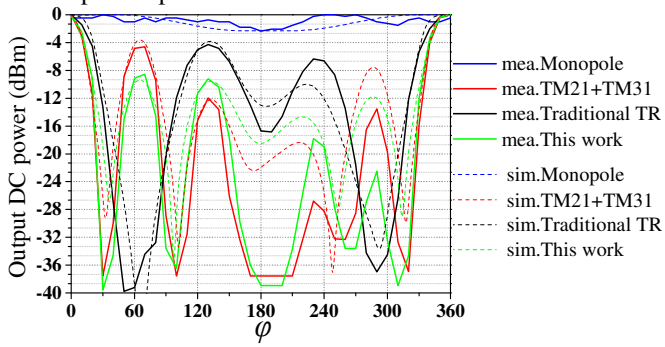

Fig. 11 Normalized simulated and measured power distribution of $\varphi_{aim} = 0°$ over a 360° range

TABLE I

COMPARISON OF DIFFERENT METHODS

Method	Power of main lobe /dBm	Power of Side lobe /dBm	SLL/dB
TM21+TM31	2.15	-2.45	-4.6
Monopole	-6.06	-6.06	0
Traditional	4.34	0.05	-4.29
This work	3.53	-5.04	-8.57

Fig. 11 shows the normalized simulated and measured power distribution of $\varphi_{\text{aim}} = 0°$ over a 360° steering range. The measured angles are selected within the angles from 0° to 360° sampled at an interval of 10°. The proposed approach achieves the lowest SLL of -8.57 dB, which is 3.97 dB lower than TM21+TM31 and 4.28 dB lower than traditional TR. It can also be seen that although the traditional TR-MPT increases the level of main lobe and reduces the *A*_high, the *A*_low becomes higher than the original *A*_high, so that the SLL of the traditional TR is -4.29 dB which is worse than the SLL of TM21+TM31 as shown in Table I. Additionally, the measured power distribution of monopole is almost same over a 360° range, which cannot form a power beam to achieve MPT with selectivity, safety and low side lobe. The simulation and measurement curves coincide well, which demonstrate the effectiveness of the proposed approach in achieving the low side lobe level.

Fig. 12 shows the normalized simulated and measured power distribution at different target angles within a 360° range. It can be seen from Fig. 11 that the proposed approach accurately focuses the power beam to the receiver of any target angle within 360°, which proves the effectiveness of the proposed approach in achieving a 360°-beam-steering auto-focus MPT. The proposed approach has an average SLL of -8.13 dB over a 360° steering range. These prove that the proposed approach achieves a 360° steering range and low side lobes. In addition, it is worth noting that the power of the power beams obtained by the proposed approach at different target angles within 360° fluctuates within 0.7 dB.

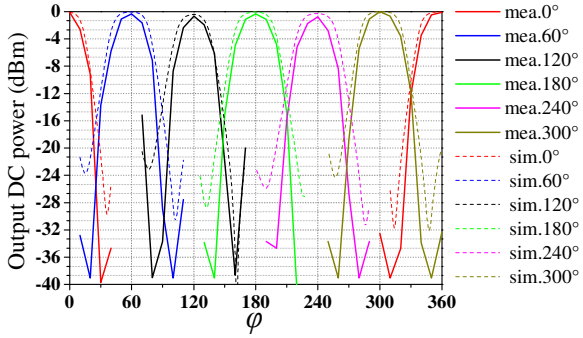

Fig. 12 Normalized simulated and measured power distribution at different target angles within a 360° steering range.

TABLE II

COMPARISON OF THE RELATED MPT SYSTEMS

Ref.	Angle /°	SLL /dB	Size /cm^2	Power fluctuation of main lobe /dB	Efficiency	Auto-focusing
[7]	±45	N/A	25×29	4.5	1.01%	YES
[8]	±40	-7*	6×31*	3	0.013%	YES
[9]	±45	N/A	27.2×27.2	3.6	0.14%	YES
[10]	±45	-6	40×60*	3	8.75%	YES
[12]	30.9	N/A	14×28*	2.4*	0.4%	YES
[13]	±10	N/A	33×33	N/A	0.28%	YES
This work	**360**	**-8.57**	π ×4.25^2	**0.7**	1.08%	YES

N/A**:** not available. *: Graphically estimated

B. Comparison with Other MPT Systems

Table II compares the critical specifications of the proposed approach with related works. Compared with systems in [7] [8] [9] [10] [12] [13], the proposed approach achieving maximum beam steering angle, smallest transmit antenna size, lowest side lobe level, smallest fluctuation of power of main lobe and auto-focusing, which paves a critical step for the practical MPT applications such as smart factories and smart homes.

IV. CONCLUSION

In this letter, we present a 360°-beam-steering low-side-lobe TR-MPT system based on the superposition of multiple weighted radiation modes in phase. The weight calculation of multiple radiation modes to achieve the lowest side lobe level was studied, and the 5-ports compact antenna supporting corresponding radiation modes was manufactured. The experimental results demonstrate that the proposed approach can not only adaptively focus the power beam at the receiver of any target angle within 360°, but also achieve the lowest sidelobe level of -8.57 dB. In addition, maximum power for different steering angles within 360° fluctuates within 0.7 dB. The results show the potential in practical MPT applications, such as wirelessly powering sensors, RFID tags, wireless headphones or smart bracelets that are distributed around the transmitter at any angle.

REFERENCES

[1] Z. Zhang, H. L. Pang, A. Georigiadis, and C. Cecati, "Wireless power transfer-an overview," *IEEE Trans. Industrial Electronics*, vol. 66, no. 2, pp. 1044-1058, Feb. 2019.

[2] Y. Zeng, B. Clerckx and R. Zhang, "Communications and signals design for wireless power transmission," *IEEE Transactions on Communications*, vol. 65, no. 5, pp. 2264-2290, May 2017.

[3] S. Assawaworrarit, X. Yu, and S. Fan, "Robust wireless power transfer using a nonlinear parity-time-symmetric circuit," *Nature*, vol. 546, no.7658, pp. 387-390, June 2017.

[4] K. W. Choi, et al., "Toward realization of long-range wireless-powered sensor networks," *IEEE Wireless Communications*, vol. 26, no. 4, pp. 184-192, Aug. 2019.

[5] Q. Hui, K. Jin, and X. Zhu, "Directional radiation technique for maximum receiving power in microwave power transmission system," *IEEE Trans. Industrial Electronics*, vol. 67, no. 8, pp. 6376-6386, Aug. 2020

[6] X. Yang, W. Geyi and H. Sun, "Optimum design of wireless power transmission system using microstrip patch antenna arrays," *IEEE Antennas and Wireless Propagation Letters*, vol. 16, pp. 1824-1827, 2017.

[7] L. Hu et al., "Auto-tracking time reversal wireless power transfer system with a low-profile planar RF-channel cascaded transmitter," *IEEE Transactions on Industrial Electronics*, vol. 70, no. 4, pp. 4245-4255, April 2023.

[8] Y. Kang, X. Q. Lin, Y. Li and B. Wang, "Dual-frequency retrodirective antenna array with wide dynamic range for wireless power transfer," *IEEE Antennas and Wireless Propagation Letters*, vol. 22, no. 2, pp. 427-431, Feb. 2023.

[9] H. Koo, et al., "Retroreflective transceiver array using a novel calibration method based on optimum phase searching," *IEEE Trans. Industrial Electronics*, vol. 68, no. 3, pp. 2510-2520, Mar. 2021.

[10] P. D. Hilario Re, S. K. Podilchak, et al, "Circularly polarized retro-directive antenna array for wireless power transmission," *IEEE Trans. Antennas and Propagation*, vol. 68, no. 4, pp. 2743-2752, Apr 2020.

[11] D. Belo, D. C. Ribeiro, P. Pinho, and N. B. Carvalho, "A selective, tracking, and power adaptive far-field wireless power transfer system," *IEEE Trans. Microw. Theory Tech.*, vol. 67, no. 9, pp. 3856-3866, Sept. 2019.

[12] X. Wang, S. Sha, J. He, L. Guo and M. Lu, "Wireless power delivery to low-power mobile devices based on retro-reflective beamforming," *IEEE Antennas and Wireless Propagation Letters*, vol. 13, pp. 919-922, 2014.

[13] B. Yang, T. Mitani and N. Shinohara, "Auto-tracking wireless power transfer system with focused-beam phased array," *IEEE Transactions on Microwave Theory and Techniques*, vol. 71, no. 5, pp. 2299-2306, May 2023.

[14] Y. Tanaka et al., "Simulation and implementation of distributed microwave wireless power transfer system," *IEEE Transactions on Microwave Theory and Techniques*, vol. 71, no. 1, pp. 102-111, Jan. 2023.

[15] B. A. Twumasi, J. -L. Li, E. T. Ashong and S. Menanor, "Circular monopole time reversal mirror for microwave wireless power transfer applications," *2021 IEEE AFRICON*, pp. 1-5, Arusha, United Republic of Tanzania, 2021.

[16] J. Parron, E. A. Cabrera-Hernandez, A. Tennant and P. de Paco, "Multiport compact stacked patch antenna with 360° beam steering for generating dynamic directional modulation," *IEEE Transactions on Antennas and Propagation*, vol. 69, no. 2, pp. 1162-1167, Feb. 2021.

[17] H. S. Park and S. K. Hong, "Investigation of time-reversal based far-field wireless power transfer from antenna array in a complex environment," *IEEE Access*, vol. 8, pp. 66517-66528, Apr. 2020.

[18] R. Ibrahim, et al., "Experiments of time-reversed pulse waves for wireless power transmission in an indoor environment," *IEEE Trans. Microw. Theory Tech.*, vol. 64, no. 7, pp. 2159-2170, June 2016.

[19] R. Garg, P. Bhartia, I. Bahl and A. Ittpiboon, "Circular disk and ring antennas," *Microstrip Antenna Design Handbook*, Norwood, MA, USA:Artech House, 2001.

[20] E. A. Cabrera-Hernández, J. Parrón and A. Tennant, "Multibeam directional secure transmission with multiport compact antenna," *2022 16th European Conference on Antennas and Propagation (EuCAP)*, pp. 1-5, Madrid, Spain, 2022.

[21] E. W. Seeley, "An experimental study of the disk-loaded folded monopole," *IRE Transactions on Antennas and Propagation*, vol. 4, no. 1, pp. 27-28, Jan. 1956.